Monatshefte für Chemie - Chemical Monthly (2022) 153:369–382
https://doi.org/10.1007/s00706-022-02908-w

ORIGINAL PAPER

An innovative approach to use zeolite as crosslinker for synthesis of p(HEMA-co-NIPAM) hydrogel

Seçil Durmuş[1] · Betül Yılmaz[1] · Alper Onder[2] · Pinar Ilgin[3] · Hava Ozay[2] · Ozgur Ozay[2,4]

Received: 29 December 2021 / Accepted: 12 March 2022 / Published online: 22 March 2022

Abstract

This study introduced a modified method to synthesize organic–inorganic hybrid crosslinker based on zeolite. First, zeolite nanoparticles were modified with 3-(aminopropyl)trimethoxysilane. Then, the amine-functionalized zeolite has been reacted with the glycidyl methacrylate via an epoxide ring-opening mechanism. The vinyl-functionalized zeolite was applied as a crosslinking agent to form hydrogel network. A novel temperature-sensitive nanocomposite hydrogel was prepared by crosslinking *N*-isopropylacrylamide as a comonomer and 2-hydroxyethyl methacrylate as a monomer with free-radical polymerization. Results showed that p(2-hydroxyethyl methacrylate-co–*N*-isopropylacrylamide)/vinyl-functionalized zeolite nanocomposite hydrogel has a chemically crosslinked and porous network structure. The content of crosslinker and monomers had obvious effects on the swelling ratio of the nanocomposite hydrogel. The temperature and salt-sensitive behavior of the hydrogels are also discussed. We offer a multifunctional crosslinker for preparing sensitive materials that can serve biomedical or environmental applications.

Graphical abstract

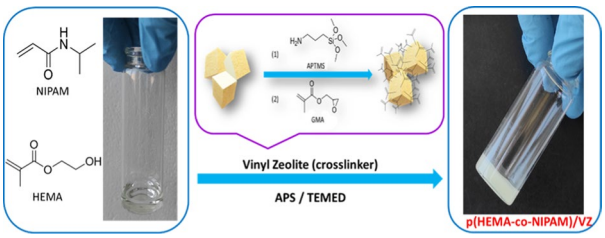

Keywords Multifunctional composites · Smart materials · Hydrogel · Zeolite

Introduction

Hydrogels are hydrophilic three-dimensional network polymer materials that are insoluble in water but can absorb large volumes of water. They have attracted great attention in the polymer literature due to their potential for a variety of applications, from biomedical applications to wastewater treatment [1–4]. Most interest in hydrogels is linked to having many adjustable physicochemical features (e.g., stiffness, pore size, elasticity, viscosity, stability, biocompatibility, degradability, surface/textural properties) [5]. In recent times, advances in nanotechnology and biotechnology have led to the design of hydrogel networks with superior features and unique functionality (e.g., high surface area, nanoscale

✉ Pinar Ilgin
pinarilgin@comu.edu.tr; pinarilgin2014@gmail.com

1 School of Graduate Studies, Department of Bioengineering and Materials Engineering, Canakkale Onsekiz Mart University, Canakkale, Turkey

2 Laboratory of Inorganic Materials, Department of Chemistry, Faculty of Science and Arts, Canakkale Onsekiz Mart University, Canakkale, Turkey

3 Department of Chemistry and Chemical Processing Technologies, Lapseki Vocational School, Canakkale Onsekiz Mart University, Lapseki, Canakkale, Turkey

4 Department of Bioengineering, Faculty of Engineering, Canakkale Onsekiz Mart University, Canakkale, Turkey

size, biological activities, low immunogenicity, ligand presentation, and nontoxicity) [5, 6]. Due to functional groups in the network, hydrogels display volume changes due to swelling or shrinking behavior in response to stimuli from the environmental conditions like temperature, pH, ion concentration, light, magnetic field, or electrical field [7, 8]. Among these, temperature-sensitive hydrogels based on copolymers of poly(*N*-isopropylacrylamide) (p(NIPAM)), the most studied thermo-sensitive polymer, were investigated in a broad range [9]. Above the low critical solution temperature (LCST) or volume phase transition temperature (VPTT) of 32–34 °C, there is a sudden and reversible volume changes from hydrophilicity to hydrophobia and this causes an external release of water molecules linked to the hydrogel. Thus, p(NIPAM) hydrogels are a perfect candidate for biomedical purposes, especially as they are able to release the substance (e.g., drug, protein) at human body temperature [10, 11]. Synthetic hydrogels based on poly(2-hydroxyethyl methacrylate) (p(HEMA)) copolymers have received special interest for biomedical applications [12]. p(HEMA) has similar physical characteristics to living tissue due to being non-toxic, having high biocompatibility, being stable and having a high-water content [13].

Zeolites are essentially three-dimensional crystalline microporous materials comprising aluminosilicates. Zeolites have cages with negative charge and pores of molecular dimensions. Additionally, they have a high surface area, ion exchange features and chemical and thermal stability. Zeolites are low-cost materials that can be easily obtained from natural sources or by synthesis [14, 15]. A range of appealing physicochemical properties such as these offers zeolite-based different materials an unrivaled potential in environmental, agricultural and industrial applications, in addition to biotechnology and medical applications [16–19]. For multifarious applications, it is possible to obtain the desired physical and chemical features with simple modifications of the zeolite surface [14]. This plays an important role in the development of zeolite-derived materials [20]. The most commonly used technique for surface functionality is silanization, a simple process that does not require special conditions or expensive equipment [21]. In particular, the surface hydroxyl groups on zeolite can react easily with 3-(aminopropyl)trimethoxysilane (APTMS), one of the silane-based coupling agents, and this may provide a good platform for diverse modifications [22–24]. Due to this reaction, amino groups are directly bound into the zeolite surfaces. Additionally, the glycidyl methacrylate (GMA) monomer with epoxide ring has low cost, is very reactive and suitable for many diverse polymerization reactions (e.g., atom transfer radical polymerization and reversible addition fragmentation chain-transfer polymerization) [25]. For this reason, it is frequently chosen for the production of functional polymers [26, 27]. Thus, to research the potential applicability of an organic–inorganic hybrid crosslinker, vinyl-functionalized zeolites (VZ) were obtained in this study for the first time to our knowledge via the ring-opening reaction of epoxy groups of GMA with the NH_2 groups of the modified zeolite surface.

This study is thought to offer an alternative to synthesis methods of hydrogels created with traditional crosslinkers [28–30] and composite hydrogels including zeolite in the network with the blending process [31–33] for the construction of clay-based crosslinked hydrogels in the future. Thus, as the multidimensional aspects of these materials with reactive functional groups which can perform comprehensive modifications of the surface increase, the aim is to obtain new-generation advanced materials offering a range of features and uses that are being newly discovered.

These new vinyl-functionalized zeolites may act as both a crosslinker unit and an element forming the matrix, obtained with a low-cost method. With the incorporation of vinyl-functional zeolites into the hydrogel network matrix, it can be expected that the thermal, stability, mechanical, functional properties would improve, and thus the network structure would improve on its own. Zeolite particles bind covalently to the matrix guaranteeing homogeneous distribution within the continuous hydrogel network. It may be possible to synthesize novel stimulant-sensitive (co)polymers with a diversity of contents and structures using VZ to produce a new hydrogel system. These (co)polymers may contribute to the development of smart materials, which are beneficial in diverse applications compared to the polymers synthesized with traditional methods (with crosslinkers) in the literature [28–33].

p(2-hydroxyethyl methacrylate-co–*N*-isopropylacrylamide)/vinyl-functionalized zeolite (p(HEMA-co-NIPAM)/VZ) nanocomposite hydrogels containing zeolite particles were characterized in a detailed and comprehensive way. The effect of experimental factors like comonomer concentration, temperature and pH of solution, and ions in water on the swelling ratio were measured and, the hydrophilic structures and swelling mechanism were investigated in detail. Surface morphology was identified with a scanning electron microscope (SEM) and transmission electron microscope (TEM). Spectroscopic and structural features were analyzed with Fourier transform infrared spectroscopy (FT-IR) and X-ray diffraction (XRD). The effect on the thermal stability of nanocomposite hydrogels obtained in the presence of zeolite was analyzed with thermogravimetric analysis (TGA). Additionally, the change in pore dimension of modified zeolite particles was investigated with Brunauer–Emmett–Teller (BET) surface area analysis.

Results and discussion

Hydrogel preparation

A schematic diagram for the method used to create vinyl-functionalized zeolite is shown in Fig. 1a. Silanol groups on the surface of zeolite particles functionalized by APTMS created a bridge suitable for epoxide opening with the GMA reagent. The general schematic diagram for the formation of p(HEMA-co-NIPAM) nanocomposite hydrogels crosslinked with the multifunctional crosslinker VZ is shown in Fig. 1b. Synthesis of p(HEMA-co-NIPAM)/VZ nanocomposite hydrogel was optimized to produce an easy-to-use hydrogel. The p(HEMA-co-NIPAM)/VZ nanocomposite hydrogel formation process begins after homogeneous distribution of monomer/crosslinker in an ultrasonic bath for a certain duration, heating to 40 °C and addition of the initiator (APS/TEMED) (Fig. S1). Detailed characterization of the crosslinking mechanism and the swelling process of hydrogels in water are exhibited. Table 1 represents the preparation conditions for the polymer/crosslinker systems in water.

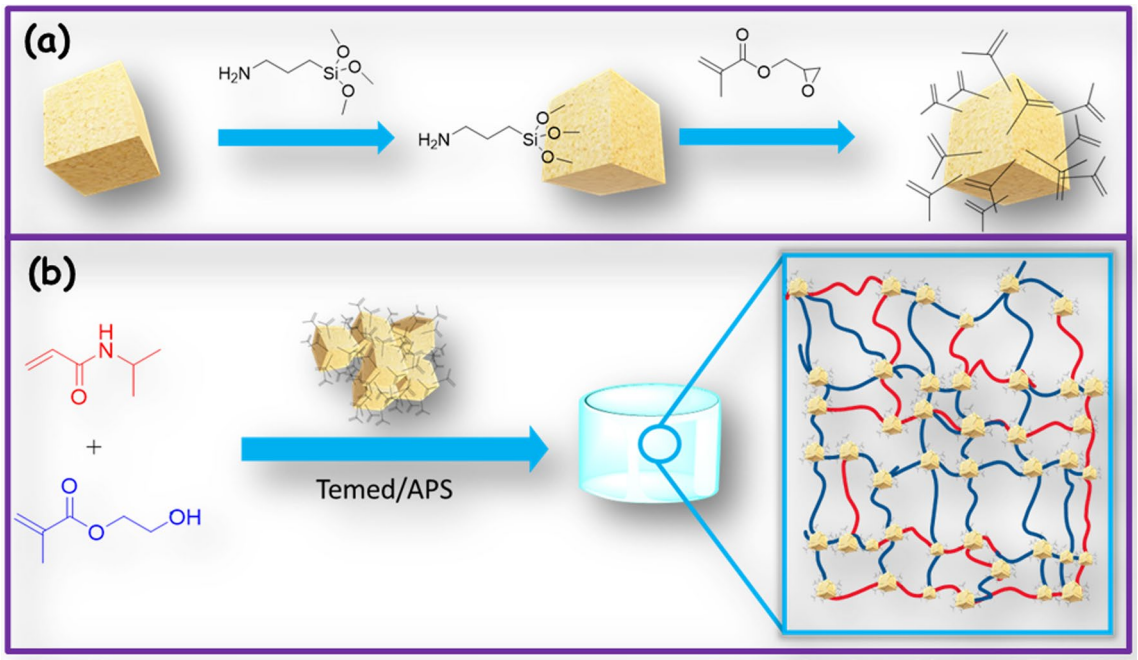

Fig. 1 Schematic diagram for the formation of **a** vinyl-functionalized zeolite particles and **b** p(HEMA-co-NIPAM)/VZ nanocomposite hydrogels

Table 1 The synthesis compositions of p(HEMA-co-NIPAM)/VZ nanocomposite hydrogels

Hydrogel	HEMA:NIPAM mole ratio	HEMA/mmol	NIPAM/mmol	VZ/mg	Gel %
p(HEMA)/VZ	100:0	17.00	0	30	91.72
p(HEMA-co-NIPAM)/VZ (75:25)	75:25	12.75	4.25	30	91.09
p(HEMA-co-NIPAM)/VZ (50:50)	50:50	8.50	8.50	30	85.68
p(HEMA-co-NIPAM)/VZ (25:75)	25:75	4.25	12.75	30	68.19
p(NIPAM)/VZ	0:100	0	17.00	30	61.58
p(HEMA-co-NIPAM)/VZ (50:50)	50:50	8.50	8.50	20	81.06
p(HEMA-co-NIPAM)/VZ (50:50)	50:50	8.50	8.50	30	85.68
p(HEMA-co-NIPAM)/VZ (50:50)	50:50	8.50	8.50	40	94.09
p(HEMA-co-NIPAM)/VZ (50:50)	50:50	8.50	8.50	50	96.12
p(HEMA-co-NIPAM)/VZ (50:50)	50:50	8.50	8.50	60	96.15

Fixed APS (1% based on total monomer mole ratio in 250 mm^3) and TEMED 30 mm^3

Distilled water was added as much as the weight of NIPAM

The copolymers synthesized using the concentrations and molar ratios for initial monomers had the following features. The p(HEMA-co-NIPAM)/VZ nanocomposite hydrogels containing 30 mg fixed crosslinker with up to 50 mol% NIPAM were easy to use and efficiently cut. As the NIPAM proportion in the hydrogel composition increased, the synthesized gels were too soft for effective processing. From this perspective, molar ratio 50:50 was determined to be optimal to produce nanocomposite copolymers and this proportion was used during the study.

SEM analysis

The SEM technique was used to compare pure zeolite and modified zeolite samples (Fig. 2a,b). All samples displayed the cubic morphology typical for zeolite. The morphology of the VZ particles is almost similar to the main zeolites (Fig. 2a), but it is clear that the surface of the vinylated zeolites (Fig. 2b) becomes rougher than the surface of the main zeolites, indicating that some frameworks have been destroyed. The porosity of the p(HEMA-co-NIPAM)/VZ nanocomposite hydrogel samples and the observation of crosslinked network structures were evaluated by SEM technique. Images for hydrogel samples in the dry state were acquired after complete swelling of the samples followed

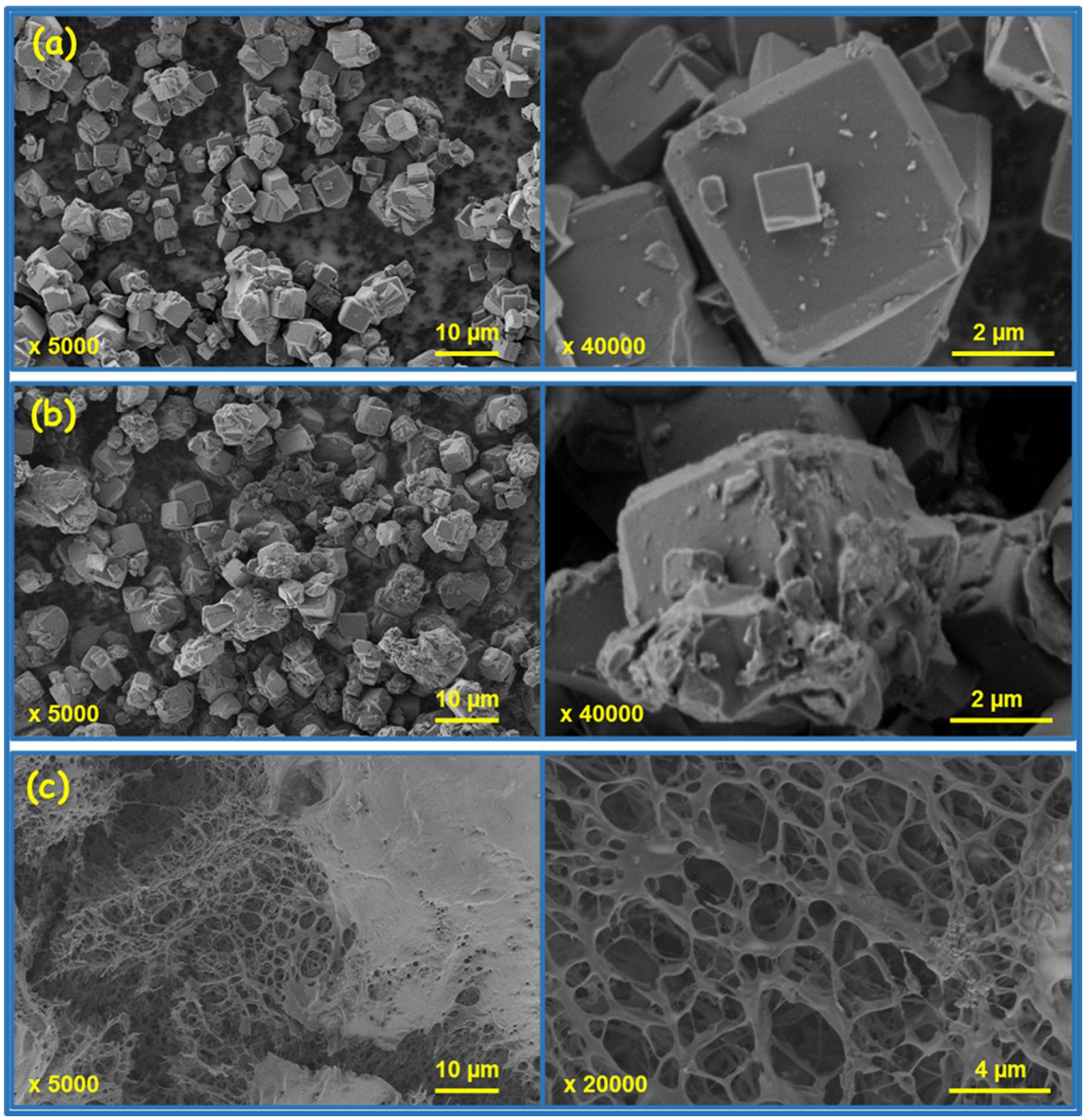

Fig. 2 SEM images of **a** pure zeolite particle, **b** vinyl-functionalized zeolite particle, and **c** p(HEMA-co-NIPAM)/VZ nanocomposite hydrogel

by lyophilization. The images in Fig. 2c confirm chemical crosslinking with VZ by observing deep cavities and pores in the copolymer chains. These cavities and holes cause large water-holding capacity linked to the increase in the contact area between water and hydrogel sample [34]. With the obtained SEM images, it was concluded that the pores in the hydrogel sample are linked to each other, and this may affect the water-holding capacity. Additionally, it is clear that the crosslinker VZ particles is uniformly distributed within the polymer matrix.

TEM and EDX analysis

Additionally, the TEM technique was used to compare modified zeolite samples with pure zeolite samples. On TEM images, some small changes to the VZ structure on the nanoscale are observed (Fig. 3). These changes appear to be small cluster-like grains on the particle surfaces due to the formation of an organic layer on the surface of the modified zeolite when compared with the unmodified zeolite. At the same time, the efficacy of modification was confirmed with EDX analysis. EDX analysis was completed to research the basic composition of the synthesized VZ samples and additionally confirm the inclusion of APTMS in the zeolite structure. As seen in Fig. 3c, peaks belonging to C, O, Al, Si, and N are present. The height of the peaks shows the amount of each element in the VZ sample. Additionally, the presence of N peak in this model confirms the modification of zeolite.

FT-IR analysis

On Fig. 4a, there are FT-IR spectra for (A) GMA, (B) the silane-crosslinking agent (APTMS), and (C) pure zeolite. Figure 4b shows the FT-IR spectra for ZA (D) and VZ (E). In spectrum (A), the peaks at 1716, 1638, and 907 cm^{-1} are peaks assigned to the C=O, C=C, and epoxy rings in the GMA structure, respectively. The peaks at 2940 and 2840 cm^{-1} on spectrum (B) are the C-H asymmetric and symmetric stretching in the methyl group, respectively, while the peaks at 805 and 776 cm^{-1} show the presence of

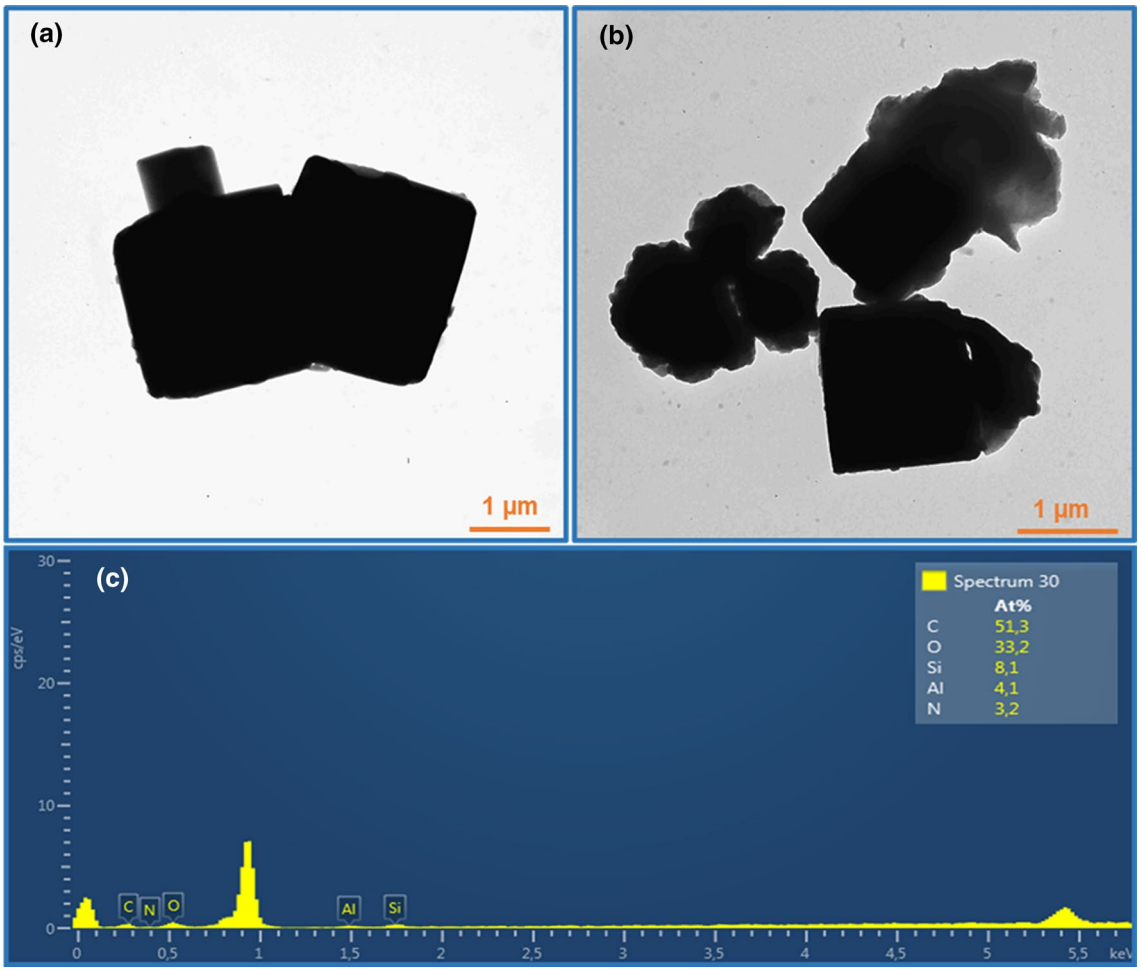

Fig. 3 TEM images of **a** pure zeolite particle, **b** vinyl-functionalized zeolite particle, and **c** EDX analysis of vinyl-functionalized zeolite particle

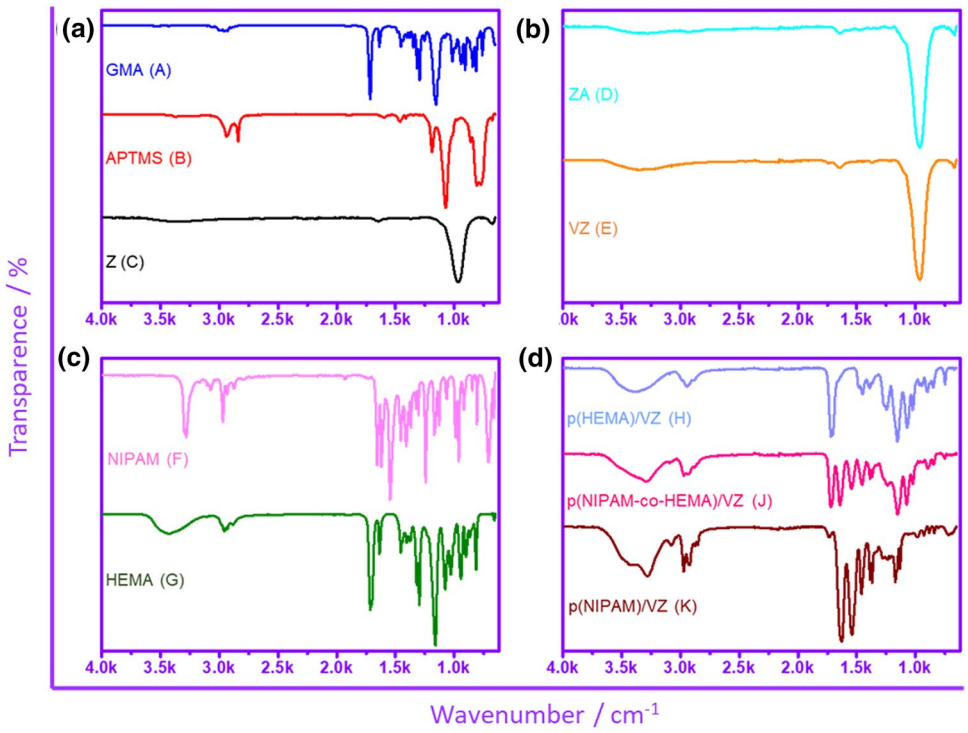

Fig. 4 FT-IR spectra of **a** GMA (A), APTMS (B), and pure zeolite (C); **b** ZA (D) and VZ (E); **c** NIPAM monomer (F), HEMA monomer (G); **d** p(HEMA)/VZ (H), p(HEMA-co-NIPAM)/VZ (J), and p(NIPAM)/VZ (K) nanocomposite hydrogel

methoxysilane ($Si-O-CH_3$) groups. The two peaks at 1464 and 1414 cm^{-1} labeled as belonging to NH_2 shear vibrations show the presence of the NH_2 terminal group of APTMS. In spectrum (C), a very broad absorption band centered at 3600–3000 cm^{-1} was observed, which was assigned to silanol groups (Si–OH) on the surface of the zeolite. The bands at 966 and 671 cm^{-1} represent asymmetric stretching and bending of siloxane groups (Si–O) [35, 36]. Spectrum (D) is observed to have new tiny peaks from 1600 to 1400 cm^{-1} showing the zeolite structure after the silanization process (Fig. S2). These peaks are accepted as vibrations of the aliphatic amine (N–H) groups. This FT-IR result shows that the silanization reaction successfully changed the surface of the zeolite without changing the zeolite structure. Finally, in the spectrum (E), the most pronounced peak confirming the inclusion of GMA in the silanized zeolite structure is attributed to C=O group observed at 1738 cm^{-1}. Additionally, further evidence of vinyl functionality is the overlap of molecular water internal stretching and bending vibration modes observed at nearly the same vibrations for stretch frequency as the 1647 cm^{-1} peak belonging to the C=C group (Fig. S2).

Figure 4c shows the FT-IR spectra for (F) NIPAM monomer, (G) HEMA monomer, and Fig. 4d shows the FT-IR spectra for (H) p(HEMA)/VZ, (J) p(HEMA-co-NIPAM)/VZ, (K) p(NIPAM)/VZ nanocomposite hydrogel. Due to polymerization and crosslinking processes in the hydrogels, significant differences are observed in the absorption maxima on the FT-IR spectra. The HEMA monomer (spectrum G) contains the typical double bond at 1634 and 816 cm^{-1} (–C=C–), while the p(HEMA)/VZ nanocomposite hydrogel (spectrum H) shows the –C=C– bonds are consumed and lost during the crosslinking reaction with VZ. Additionally, similar peaks like –OH (3100–3600 cm^{-1} broad band), –C=O (1715 cm^{-1}), –C–O–C– (1157 cm^{-1}), $-CH_2$ (1484–1359 cm^{-1}) are present in both spectra [37]. As can be clearly seen from bands observed at 966 (Si–O), the presence of VZ is notable. When the FT-IR spectra for NIPAM monomer (spectrum F) and p(NIPAM)/VZ nanocomposite hydrogel (spectrum K) are compared, several variations may be observed. The first difference in the spectra is at 3700–3100 cm^{-1}. In this section of the monomer spectrum, the absorption peak for NH vibration is observed at 3280 cm^{-1}, while this peak is much broader in the hydrogel spectrum due to the overlap with the characteristic absorption peak for –OH vibrations of bound-water molecules due to the interaction of the polymer molecules with adjacent water molecules [38]. The FT-IR spectrum for the NIPAM monomer has typical peaks equivalent to amide I (1656 cm^{-1}), amide II (1545 cm^{-1}, isopropyl group (1384 and 1366 cm^{-1}), and vinyl group (1617, 1407, 807 cm^{-1}). During radical polymerization of the NIPAM, the characteristic peaks (C=C) for vinyl groups are lost. The peaks for amide I (1630 cm^{-1}) and amide II (1538 cm^{-1}) groups are offset in the p(NIPAM) spectrum. As can be clearly seen from bands observed at 1730 (–C=O) and 982 (Si–O), the presence of VZ is clearly noted. For the copolymer (spectrum J), the presence of clear characteristic peaks for C=O

(1716) from HEMA and amide I (1640 cm^{-1}), amide II (1542 cm^{-1}), and 993 (Si–O) from NIPAM is notable. Additionally, no new peak emerges showing no new molecular chemical bonds or structures formed during the crosslinking reactions with VZ for p(NIPAM)/VZ and p(HEMA)/VZ homopolymers and copolymers. The results show that VZ fulfilled its task as a crosslinker and was included in the polymer network structures. Additionally, p(HEMA), p(NIPAM) homopolymers, and p(HEMA-co-NIPAM)/VZ copolymers were successfully synthesized with the radical polymerization method.

Thermogravimetric analysis

The thermal stability of crosslinked p(HEMA-co-NIPAM)/VZ composite polymer was researched with thermogravimetric analysis (TG/DTG) (Fig. 5). The sample was observed to undergo three stages of degradation. The polymer sample was observed to have ~15% initial weight loss before ~300 °C linked to bound-water molecules and low volatile impurities. Later, the highest weight loss of ~78% occurred at temperatures from 300 to 475 °C. In this curve where the main degradation occurred, the crosslinker polymer structure was broken and the polymer chains are considered to degrade. In the final degradation step, ~5% final mass loss began at 475 °C and reached a horizontal asymptote at 720 °C. On the DTG graph, the polymer was observed to have a large degradation peak at ~375 and 450 °C. Jain et al. (2020) reported the main degradation occurred in the p(HEMA-co-NIPAM) hydrogel crosslinked with MBA at 300–445 °C with ~85% weight loss [39]. Hereby, the TGA results for p(HEMA-co-NIPAM) hydrogel crosslinked with VZ are compatible with those reported. The TGA results show that p(HEMA-co-NIPAM)/VZ nanocomposite hydrogel has high thermal stability.

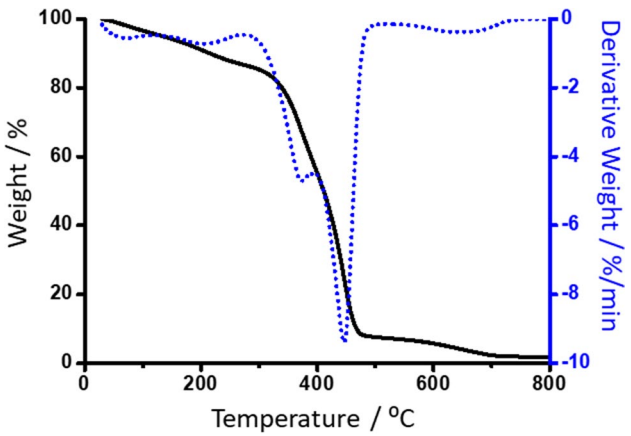

Fig. 5 Thermogravimetric analysis of p(HEMA-co-NIPAM)/VZ nanocomposite hydrogel

BET analysis

BET methodology is one of the essential parameters in terms of changes to the surface area and pore volume of material as a result of modification; for this reason, it is commonly used for predictions. A summary of the BET results for pure and vinyl-functionalized zeolites is listed in Table 2. As can be seen, when zeolite was first modified with APTMS and then GMA, both the BET surface areas and total pore volumes showed a significant degree of reduction to nearly half of the initial values. However, the pore radius values significantly increased. This confirmed the functionalization of the pure zeolite surface. In similar results, Sanaepur et al. reported that the zeolite volumes decreased by about half of the initial values with the silylation reaction [35]. Additionally, the particle size distribution results for pure and silanized zeolites were found to have larger particle size with the modification reaction. Wang reported that the specific surface area was 57.65 $m^2\ g^{-1}$ for unmodified zeolite samples and fell to 10.93 $m^2\ g^{-1}$ for functionalized zeolite [36]. According to both surface area (BET and micropores) and BET results (micro and total pores), the results of the modification process were comparable with the literature.

XRD analysis

XRD analysis was performed for advanced structural assessment of the synthesized nanocomposite hydrogels and additionally to confirm the successful inclusion of VZ within the nanocomposite hydrogel structure. XRD diffractograms for pure zeolite and zeolite modified firstly with silane and then with GMA are presented in Fig. 6a and b, respectively.

Table 2 BET results of pure and vinyl functionalized zeolite sample

Sample	BET surface area[a]/$m^2\ g^{-1}$	Adsorption pore volume[b]/$cm^3\ g^{-1}$	Total pore volume[a]/$cm^3\ g^{-1}$	Surface area[b]/$m^2\ g^{-1}$	Adsorption average pore radius[b]/nm
Zeolite	1.385	0.006	2.841×10^{-03}	3.724	1.9374
VZ	0.751	0.002	1.127×10^{-03}	0.436	3.315

[a]Multi-point desorption total pore volume of pores less than 20 nm radius width at $p/p^0 = 0.95$

[b]BJH adsorption method calculated by the multipoint BET

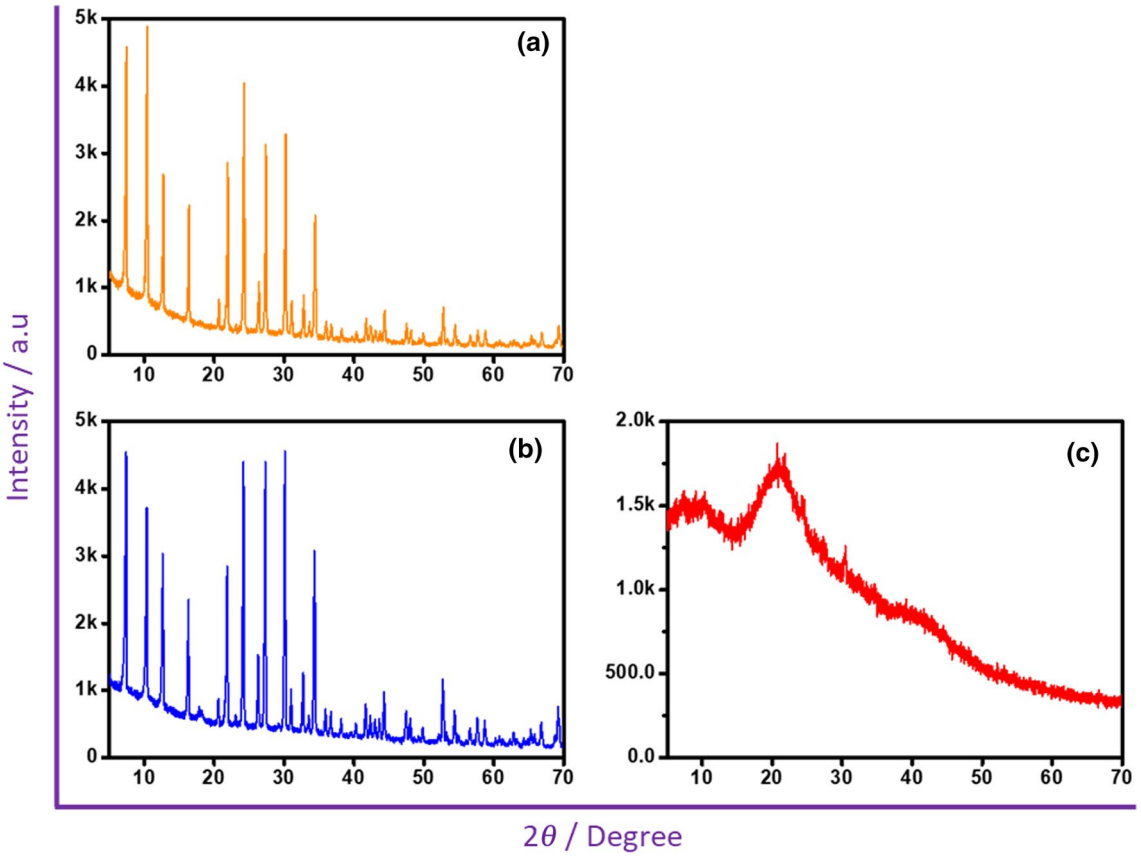

Fig. 6 XRD diffractograms of **a** pure zeolite particle, **b** vinyl-functionalized zeolite particle and **c** p(HEMA-co-NIPAM)/VZ nanocomposite hydrogel

Additionally, the XRD diffractogram for p(HEMA-co-NIPAM)/VZ nanocomposite hydrogel is given in Fig. 6c. The VZ diffractograms display clearly similar patterns to pure zeolite. However, the crystal structure of the zeolite slightly changes during surface modification, and this causes a slight elevation in the peak intensity. After the VZ particles are included in the polymer, the XRD patterns show the characteristic peaks for both, confirming crosslinking. The p(HEMA-co-NIPAM)/VZ nanocomposite hydrogels gain an amount of crystallinity in the presence of zeolite. The broad peak centered at $2\theta \sim 10°$ and $\sim 22°$ confirms the amorphous structure of the polymer. Additionally, the small peaks observed around $\sim 30°$ in the polymer XRD model show it is crystalline. Finally, it should be stated that the crystallinity of the zeolite does not have a significant effect and nanocomposite hydrogel sample with amorphous structure was obtained.

Swelling studies

The swelling ratio (S) is vital in terms of the usability of hydrogels in practical applications like sensors, adsorbents or drug-carrier materials. The affinity of hydrogels for water is known to be associated with a variety of factors like the structure of the polymer chains, density of crosslinks in the polymer chain network, ionic osmotic pressure, environmental temperature and solvent–solute interactions.

Effect of crosslinker amount on the swelling ratio

Figure 7a shows the variation in % equilibrium swelling ratio for copolymer hydrogels produced with 50/50 molar ratio of HEMA and NIPAM at the end of 24 h at room temperature (26 °C) linked to the VZ-crosslinker content. The equilibrium swelling ratio increased with crosslinker content from 20 to 40 mg and reduced after 40 mg. In general, it is known that the hydrogel exhibits a lower ratio of equilibrium swelling, as the increased crosslink density in a hydrogel has the effect of increasing the resistive force against the elongation of monomer chains [40]. However, a reasonable explanation for this behavior is that it may be due to the water-absorption capacity of zeolite, in addition to the polymer network responsible for holding water. With VZ content up to 40 mg as crosslinker in the network structure, the hydrophilic group concentration in the network structure increased; this significantly contributed to improving

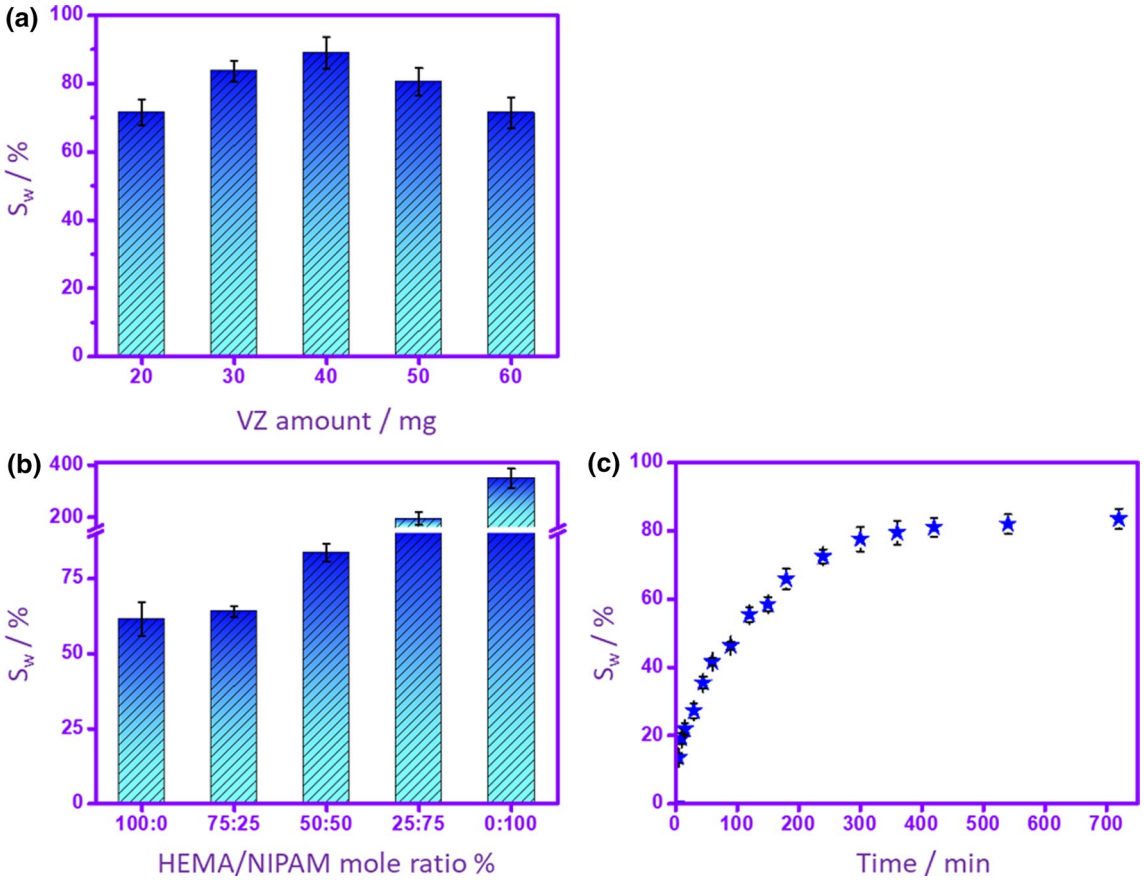

Fig. 7 **a** Swelling ratio of p(HEMA-co-NIPAM)/VZ (50:50) nanocomposite hydrogel vs varying crosslinker amount, **b** swelling ratio of p(HEMA-co-NIPAM)/VZ (30 mg VZ) nanocomposite hydrogel vs. HEMA/NIPAM monomer mole ratio, **c** swelling ratio curve of p(HEMA-co-NIPAM)/VZ (50:50) (30 mg VZ) nanocomposite hydrogel vs time

the percentage swelling [41, 42]. Additionally, the swelling capacity was reduced with the increase in VZ amount. The reason for this may be the increase in covalent crosslinker points in addition to the formation of physical crosslinker bonds in the hydrogel matrix. This situation may cause difficulty in water molecules infiltrating the internal structure of the hydrogel [31]. In addition, increasing the crosslink content may have increased the gel fraction by an increase in the presence of active primary radical (Table 1).

Effect of monomer ratio on the swelling ratio

The % equilibrium swelling ratio for nanocomposite hydrogels produced at varying HEMA/NIPAM mole ratios was researched at room temperature (26 °C) for 24 h (Fig. 7b). While the p(NIPAM)/VZ nanocomposite hydrogel had the highest swelling ratio, p(HEMA)VZ nanocomposite hydrogel had the lowest swelling ratio. The swelling ratio for copolymer hydrogels produced with different HEMA/NIPAM molar ratios was between these values. As the NIPAM content in the copolymer increased, the swelling ratio for the copolymers increased. Also, the gel fraction of the hydrogel decreased with increasing NIPAM content (Table 1), indicating the looser gel structure. The looser network structure may have increased the hydrogel's affinity for water [43]. In Fig. 7c, p(HEMA-co-NIPAM)/VZ (50:50) nanocomposite hydrogel increased swelling percentage over time and the equilibrium swelling was 83.3% and reached in 7 h.

Effect of pH value on the swelling ratio

Figure 8a shows the % equilibrium swelling ratio for p(HEMA-co-NIPAM)/VZ (50:50) nanocomposite hydrogels at the end of 24 h according to variation in pH at room temperature (26 °C). The swelling behavior of hydrogels is unexpected as they do not contain ionizable groups. The slight increase in swelling at pH 2 and 12 may be due to the breaking of some hydrogen bonds in the hydrogel network structure at lower and higher pH, resulting in more absorption of water [39]. Don et al. [44] and D'Agostino et al. [45] prepared p(NIPAM) and p(HEMA) hydrogels, respectively

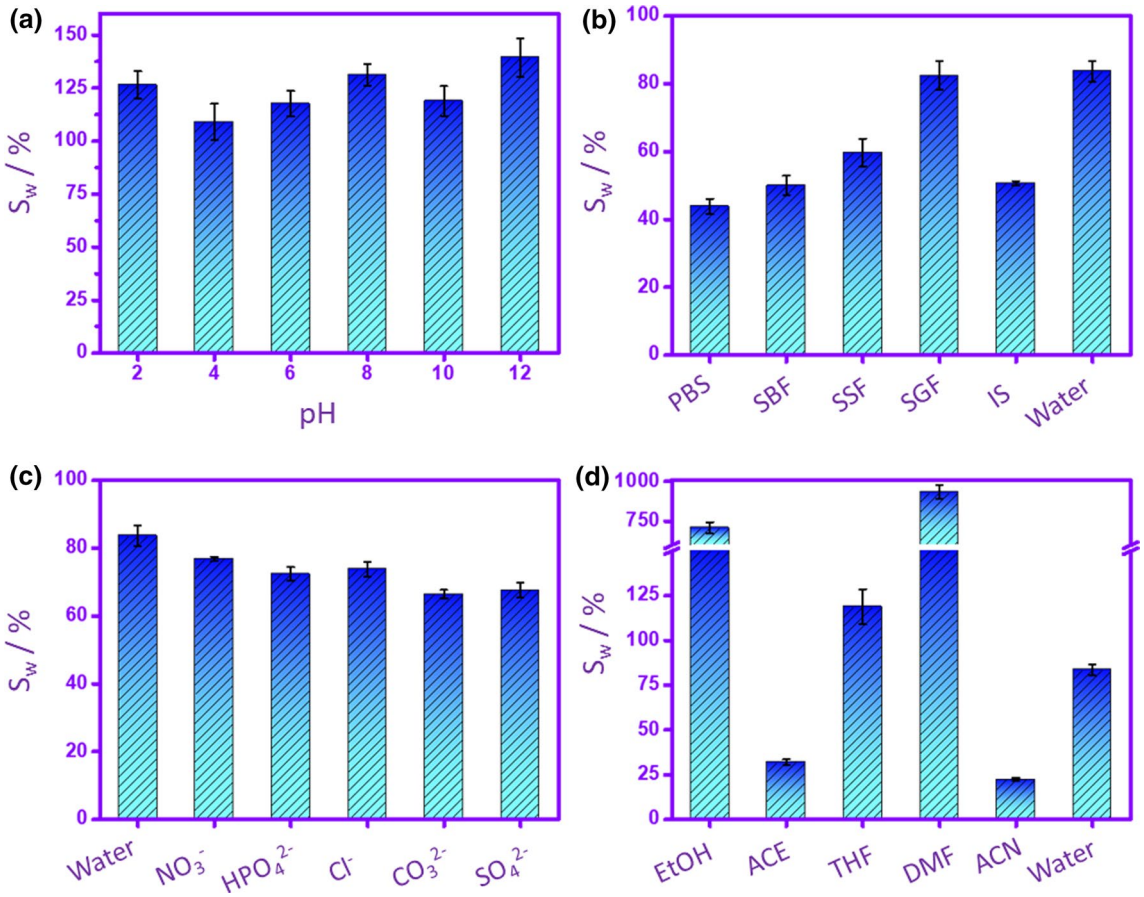

Fig. 8 Swelling ratio curve of p(HEMA-co-NIPAM)/VZ (50:50) (30 mg VZ) nanocomposite hydrogel in various **a** pH, **b** simulated solution, **c** ionic solution, **d** solvent

and found the swelling behavior of the prepared hydrogels was independent of the medium pH. However, the presence of zeolite may increase the swelling properties of the nanocomposite at medium pH of 8. This may be due to the fact that silanol groups on the zeolite surface are deprotonated at basic pH, creating repulsions between groups of SiO^- [46].

Effect of simulated solution on the swelling ratio

Figure 8b investigated the swelling ratio for p(HEMA-co-NIPAM)/VZ (50:50) nanocomposite hydrogel by dipping in various simulated solutions for 24 h at room temperature (26 °C). The results showed significant swelling capacity differences. Due to the non-ionic structure of p(HEMA) and p(NIPAM), the copolymer hydrogels are not sensitive to pH at a significant level, so the changes in swelling may be mainly due to the effect of ionic power. With the presence of soluble agents in the swelling medium, the swelling behavior of hydrogel samples can be determined by ionic interactions between fixed charges and mobile ions that change the osmotic pressure. The swelling of hydrogels may reduce due to the increase in osmotic pressure of solution ions and the reduction in Donnan osmotic pressure [47].

Effect of various salt solutions on swelling ratio

Figure 8c shows results of 0.01 M sodium salt solutions at room temperature in a variety of electrolytes to investigate the effect of anions on the % equilibrium swelling ratio of p(HEMA-co-NIPAM)/VZ (50:50) nanocomposite hydrogels. When the equilibrium swelling of hydrogels is examined, the maximum swelling was affected by the anion species though great differences are not observed. For anions, the hydrogel swelling ratio increased in the order of $CO_3^{2-} < SO_4^{2-} < HPO_4^{2-} < Cl^- < NO_3^-$. The equilibrium swelling behavior followed the Hofmeister effect [48].

Effect of various solvent on the swelling ratio

The % equilibrium swelling ratio for p(HEMA-co-NIPAM)/VZ (50:50) nanocomposite hydrogels in a variety of solvents with a variety of dielectric constants (ε) and polarities (p) is shown in Fig. 8d. Swelling was measured in different

polar aprotic solvents like tetrahydrofuran (THF, $\varepsilon = 7.52$, $p = 0.207$), acetone (ACE, $\varepsilon = 21.3$, $p = 0.355$), dimethyl formamide (DMF, $\varepsilon = 38.25$, $p = 0.386$), acetonitrile (ACN, $\varepsilon = 36.6$, $p = 0.460$) and polar protic solvents like ethanol (EtOH, $\varepsilon = 25.3$, $p = 0.654$) and water ($\varepsilon = 80.0$, $p = 1.0$) at room temperature [49]. The results show that despite EtOH having the highest polarity, the swelling was highest in DMF (highest dielectric constant). Slight swelling was observed in THF, ACE, and ACN. The hydrogel also swelled in water; however, the swelling ratio was nearly 84%. THF has a lower dielectric constant and polarity compared to ACN. Another notable result inferred from Fig. 8d is the lack of significant difference between the results obtained for ACE and ACN. Although solvents have similar properties such as polar aprotic, dielectric constants, and polarity, the solvent response of p(HEMA-co-NIPAM)/VZ (50:50) nanocomposite hydrogels is different. ACE and DMF solvents have similar polarity, and DMF and ACN solvents have similar dielectric constants but exhibit different swelling behavior. For this reason, it appears the polar character of ACE has no effect related to the swelling capacity. This shows that the dielectric constant or polarity is not suitable to describe swelling in these systems. Similarly, Pan showed that the solvent parametric approach is not universally applicable to describe the swelling of all gels in various solvents [50]. The significant differences in the swelling volume of p(HEMA-co-NIPAM)/VZ (50:50) nanocomposite hydrogels in the interval of tested solvents may be due to differences in the interaction between the hydrogel matrix and solvent molecules and the difference between solubility parameters. Especially in interactions between polymer chains and solvents, steric prevention of methyl groups disrupts polymer and hydrogen bond formation [49]. These results show that different solvents may be a good choice for drug loading by considering that water-insoluble medications are generally hydrophobic.

Effect of temperature on the swelling ratio

Figure 9a shows the effect of temperature on the % equilibrium swelling ratio for p(HEMA-co-NIPAM)/VZ (50:50) nanocomposite hydrogels. As expected, as the temperature increases, the percentage equilibrium swelling is reduced. The results showed a large decrease in swelling after 25 °C and unchanged after 45 °C. Generally, significant changes occur in p(NIPAM) at ~ 32. However, most of the shrinking of copolymer hydrogel occurred below the VPTT temperature of p(NIPAM). The reason for this is the amide group on NIPAM creates a hydrogel bond with molecules in surrounding water at low temperature and the increase in hydrophobic forces at high temperature causes phase separation of polymers [51–53]. In addition, the fact that the phase transition temperature in copolymer hydrogels takes place before 32 °C may be due to the fact that the swelling in the hydrogel depends on the crosslink density, the interaction phenomenon between the crosslinking agent molecules and the polymer chains, and the presence of HEMA that forms hydrogen bonds [39].

Figure 9b shows the deswelling behavior of p(HEMA-co-NIPAM)/VZ (50:50) nanocomposite hydrogels at 25 and 37 °C when left to dry in an oven. Rapid water release was observed at 37 °C. The results show that copolymeric hydrogels display early drying behavior from swollen form at higher temperatures. The reason for this is the amide group in NIPAM in the copolymer creates an intermolecular hydrogen bond with surrounding water at low temperature that can transform into an intra-molecular hydrogel bond above the gel transition temperature. Thus, the state of the water molecules in the hydrogel's changes from bound water to free water [51–53].

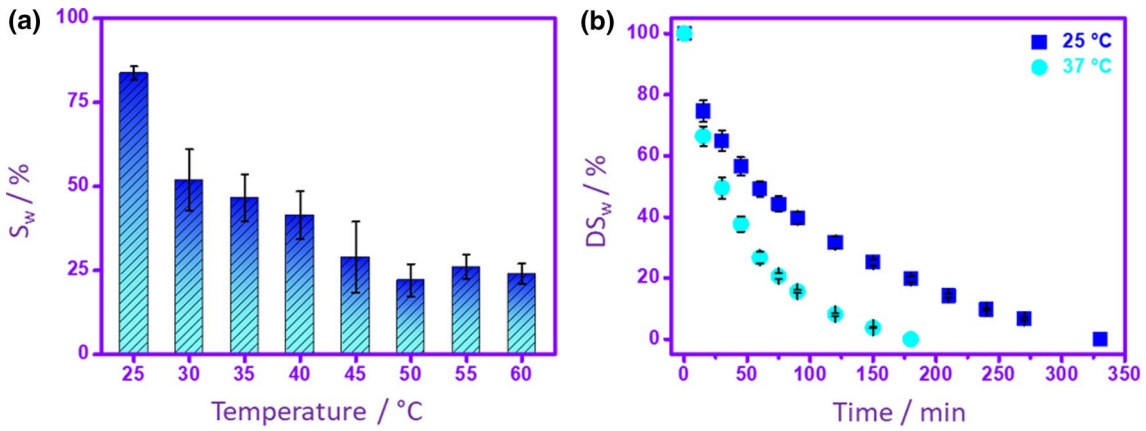

Fig. 9 **a** Shrinkage curve of p(HEMA-co-NIPAM)/VZ (50:50) (30 mg VZ) nanocomposite hydrogel vs. temperature. **b** Deswelling curve of p(HEMA-co-NIPAM)/VZ (50:50) nanocomposite hydrogel at 25 °C and 37 °C

Conclusion

In this study, a convenient preparation method was systematically investigated to produce a new clay-based nanocomposite hydrogel without conventional crosslinkers. A temperature sensitive p(HEMA-co-NIPAM)/VZ nanocomposite hydrogel was synthesized by free radical polymerization, using HEMA as starting material, NIPAM as functional monomer, vinyl-functional zeolite as crosslinker and APS as initiator. FT-IR spectra of p(HEMA-co-NIPAM)/VZ showed characteristic peaks of HEMA and NIPAM monomers and VZ crosslinker, thus confirming crosslinking of the synthesized hydrogel. Also, SEM images showed that p(HEMA-co-NIPAM)/VZ nanocomposite hydrogel has a porous network structure. Detailed swelling tests in various media were applied to the hydrogels. By varying the VZ ratio, hydrogels with different crosslinking densities can be obtained. Higher crosslinker concentration resulted in lower swelling rate. Since the hydrogels do not have an ionic structure, no significant swelling changes were observed in the solution pH and various salt solutions. When the swelling changes of the hydrogel across multiple solvent environments were examined, solvent-induced volume-phase transitions were observed. By varying the monomer ratio, hydrogels with different LCST values can be obtained. A decrease in swelling was observed with the increase in temperature. We think these new nanocomposite hydrogels can replace conventional hydrogels due to the enormous value of practical obtaining.

Experimental

Monomers (2-hydroxyethyl methacrylate (HEMA, 98%, *v*), *N*-isopropylacrylamide (NIPAM, 97%, *w*), initiator (ammonium persulfate, APS, ≥ 98%, *w*) and accelerator used for nanocomposite hydrogel synthesis (*N*,*N*,*N*′,*N*′-tetramethylethylenediamine, TEMED, 98%, *v*) were obtained from Sigma-Aldrich chemical Co. Ltd.. Zeolite (*Z*, particle size < 20 µm), 3-(aminopropyl)trimethoxysilane (APTMS, 97%, *v*), glycidyl methacrylate (GMA, 97%, *v*), and anhydrous dichloromethane used for the synthesis of vinyl zeolite crosslinker particles (VZ) were obtained from Sigma-Aldrich and Merck. All experiments, including hydrogel synthesis and swelling studies, were performed using distilled water. All experiments were repeated three times during the study.

Instruments

For the structural characterization of VZ particle, p(HEMA-co-NIPAM)/VZ nanocomposite hydrogel and other components, FT-IR spectra obtained with Perkin Elmer brand spectrometer with ATR apparatus in the range of 650–4000 cm^{-1} were used. JEOL TEM-1400-EDX model Transmission Electron Microscopy- energy-dispersive X-ray spectroscopy (TEM–EDX) was used for the internal structure analysis of the VZ particle. FEI Quanta FEG 250 model scanning electron microscope (SEM) was used for surface morphology analyzes of zeolite particle, VZ particle and lyophilized p(HEMA-co-NIPAM)/VZ nanocomposite hydrogel. The Brunauer–Emmett–Teller (BET) surface area of VZ particle was determined using the Quantachrome Quadrasorb SI instrument. The degassing temperature and time were 100 °C and 4 h, respectively. The thermal analysis of p(HEMA-co-NIPAM)/VZ nanocomposite hydrogel was performed with a Perkin Elmer brand TGA 8000 model under nitrogen gas, at a heating rate of 10 °C/min at the range of 30–800 °C. XRD analysis of Zeolite particle, VZ particle and p(HEMA-co-NIPAM)/VZ nanocomposite hydrogel were performed with PANalytical Empyrean model X-Ray Diffraction (XRD). Hanna Edge pH meter was used to prepare various pH solutions to determine the effect of pH on swelling.

Surface functionalization of zeolite particles

The synthesis of vinyl-functionalized zeolite particles was carried out in two steps. For the amine functionalization of zeolite in the first step, 1 g of zeolite was mixed in 5 cm^3 of anhydrous dichloromethane at ambient conditions for 30 min on a magnetic stirrer. At the end of the period, 1 cm^3 of APTMS was added to the mixture. The mixture was left to stir for 24 h. The white solid was separated by centrifugation and repeatedly washed with dichloromethane [54]. For the synthesis of VZ particles with the second step, 10 cm^3 of anhydrous dichloromethane solution was added to the amine-functionalized zeolite (ZA) obtained in the first step and stirred for 1 h at ambient conditions. At the end of the period, 1 cm^3 of GMA was added to the mixture and the mixture was left to stir for 24 h. The white solid was separated by centrifugation and washed three times with dichloromethane and left to dry in a desiccator at 24 h. The resulting VZ particles were stored in a desiccator for use in the synthesis of nanocomposite hydrogels.

Preparation of nanocomposite hydrogels

Similar to our previous studies, p(HEMA)/VZ nanocomposite hydrogel and p(NIPAM)/VZ nanocomposite hydrogel and p(HEMA-co-NIPAM)/VZ with 25:75, 50:50, 75:25 molar

ratio nanocomposite hydrogels that are containing fixed 30 mg VZ crosslinker particles and p(HEMA-co-NIPAM)/VZ (50:50) nanocomposite hydrogels containing varying ratio (20, 30, 40, 50, and 60 mg) of VZ crosslinker particles were prepared by the radical polymerization method (Table 1) [55, 56]. Briefly, for the synthesis of p(HEMA-co-NIPAM)/VZ (50:50) nanocomposite hydrogels, 8.5 mmol NIPAM (1.0 g in 1.0 cm^3 distilled water) and 8.5 mmol HEMA (1.13 cm^3) were dissolved in a glass vial. 30 mg of VZ crosslinker and accelerator (TEMED, 30 mm^3) were added to the reaction mixture and left in an ultrasonic bath for 30 min to homogenize the VZ crosslinker particles in the mixture. Then, the initiator (APS, 1% based on total monomer mole ratio) was dissolved in 0.25 cm^3 distilled water and added to the reaction mixture to initiate the polymerization reaction at 40 °C. It was left for 24 h for the polymerization reaction to complete. The resulting p(HEMA-co-NIPAM)/VZ nanocomposite hydrogels were cut in square form. The synthesized nanocomposite hydrogels were washed in deionized water during 24 h by changing the water every 8 h. Hydrogels were dried in a vacuum oven at 35 °C for 3 days and stored in a desiccator.

Swelling studies of nanocomposite hydrogels

The swelling behavior of the p(HEMA-co-NIPAM)/VZ (50:50) nanocomposite hydrogels in various simulated media like phosphate buffer saline (PBS, pH = 7.0), simulated body fluid (SBF, pH = 7.4), simulated saliva fluid (SSF, pH = 7.4), simulated gastric fluid (SGF, pH = 1.2), isotonic solution (IS, 0.9% NaCl, pH = 7.0), various pH conditions (2, 4, 6, 8, 10, 12), various solvent like ethanol (EtOH), acetone (ACE), tetrahydrofuran (THF), dimethylformamide (DMF), and acetonitrile (ACN) and various ionic solutions of sodium salt, 0.01 M (SO_4^{2-}, NO_3^-, CO_3^{2-}, Cl^-, HPO_4^{2-}).

The components of simulated solutions used in swelling experiments are as follows; PBS: 2.59 g KH_2PO_4 and 4.3 g Na_2HPO_4 in 0.5 dm^3 of distilled water; SBF: 4.018 g NaCl, 0.115 g KH_2PO_4, 0.176 g $NaHCO_3$, 0.1125 g KCl, 0.1555 g $MgCl_2{\cdot}2H_2O$, 0.1465 g $CaCl_2$, 0.036 g Na_2SO_4, 3.0315 g Tris in 0.5 dm^3 of distilled water; SSF: 0.4 g NaCl, 0.0095 g KH_2PO_4, 1.19 g Na_2HPO_4 in 0.5 dm^3 of distilled water; SGF: 1.0 g of NaCl, 3.7 cm^3 of HCl (37%) in 0.5 dm^3 of distilled water; IS: 4.5 g of NaCl in 0.5 dm^3 of distilled water. The pH value was adjusted with 0.1 M NaOH or 0.1 M HCl solution.

The swelling behavior of p(HEMA-co-NIPAM)/VZ nanocomposite hydrogel in various media was investigated by the gravimetric method [55, 56]. For this purpose, a dry hydrogel with known initial mass (M_0) was immersed in a swelling media. The mass changes (M_t) of the hydrogel were measured at certain time intervals until equilibrium swelling was reached. During the measurements, the excess water on the surface of the hydrogel was removed with the help of filter paper. The swelling ratio (S_w %) at equilibrium was calculated using the following equation:

$$S_w\% = \left[\left(M_t - M_0\right)/M_0\right] \times 100.$$

In order to investigate deswelling behaviors, hydrogels swollen in distilled water at 25 °C for equilibrium state (M_e) are left in the open air (25 °C) and in an oven (37 °C). The mass changes of the hydrogel (M_t) were measured at certain times intervals until its dry weight (M_0) was reached. The deswelling ratio (DS_w %) was calculated using the following equation:

$$DS_w\% = \left[\left(M_t - M_0\right)/\left(M_e - M_t\right)\right] \times 100.$$

Gel fraction of nanocomposite hydrogels

The gel fraction of nanocomposite hydrogels was determined gravimetrically. First, the prepared hydrogels were dried to a constant weight (M_c). The hydrogels were then left in water for 48 h to remove the unreacted soluble fraction and finally, dried to constant weight (M_d). The gel fraction was calculated using the following equation

$$\text{Gel}\% = M_d/M_c \times 100.$$

Supplementary Information The online version contains supplementary material available at https://doi.org/10.1007/s00706-022-02908-w.

Acknowledgements The authors thank the support of the Çanakkale Onsekiz Mart University Scientific Research Coordination Unit (project number: FBA-2020-3274).

References

1. Ozay H, Ilgin P, Ozyurt C, Ozay O (2020) Polym Plast Technol Mat 59:1944
2. Guo Y, Fang Z, Yu G (2021) Polym Int 70:1425
3. Shinde DB, Pawar R, Vitore J, Kulkarni D, Musale S, Giram P (2021) Polym Adv Technol 32:4204
4. Campea MA, Majcher MJ, Lofts A, Hoare T (2021) Adv Funct Mater 31:2102355
5. Cao H, Duan L, Zhang Y, Cao J, Zhang K (2021) Sig Transduct Target Ther 6:426
6. Sikdar P, Uddin MM, Dip TM, Islam S, Hoque MS, Dhar AK, Wu S (2021) Mater Adv 2:4532
7. Irfan J, Hussain MA, Haseeb MT, Ali A, Farid-ul-Haq M, Tabassum T, Hussain SZ, Hussain I, Naeem-ul-Hassan M (2021) RSC Adv 11:19755
8. Samal SK, Dash M, Dubruel P, Vlierberghe SV (2014) Smart polymer hydrogels: properties, synthesis and applications. In: Aguilar MR, San Román J (eds) Smart polymers and their applications. Elsevier, Amsterdam, p 237
9. Ashraf S, Park H-K, Park H, Lee S-H (2016) Macromol Res 24:297
10. Chatterjee S, Hui PC-L (2021) Polymers 13:2086

11. Li Z, Liang B (2022) Polym Adv Technol 33:710
12. Ozay O, Ilgin P, Ozay H, Gungor Z, Yilmaz B, Kıvanç MR (2020) J Macromol Sci A 57:379
13. Oucif A, Haddadine N, Zakia D, Bouslah N, Benaboura A, Beyaz K, Guedouar B, El-Shall MS (2022) Polym Bull 79:1535
14. Baile P, Fernández E, Vidal L, Canals A (2019) Analyst 144:366
15. Król M (2020) Curr Comput-Aided Drug Des 10:622
16. Karimi M, Habibizadeh M, Rostamizadeh K, Khatamian M, Divband B (2019) Polym Bull 76:2233
17. Millini R, Bellussi G (2016) Catal Sci Technol 6:2502
18. Zaarour M, Dong B, Naydenova I, Retoux R, Mintova S (2014) Microporous Mesoporous Mater 189:11
19. Purnomo, Setyarini PH, Sulistyaningsih D (2018) AIP Conf Proc 1977:030013
20. Shi J, Yang Z, Dai H, Lu X, Peng L, Tan X, Shi L, Fahim R (2018) Water Sci Technol 2017:621
21. Qiao B, Wang T-J, Gao H, Jin Y (2015) Appl Surf Sci 351:646
22. Guo Y-P, Wang H-J, Guo Y-J, Guo L-H, Chu L-F, Guo C-X (2011) Chem Eng J 166:391
23. Palimi MJ, Rostami M, Mahdavian M, Ramezanzadeh B (2014) Prog Org Coat 77:1663
24. Metın D, Tihminlioğlu F, Balköse D, Ülkü S (2004) Compos A: Appl Sci Manuf 35:23
25. Muzammil E, Khan A, Stuparu MC (2017) RSC Adv 7:55874
26. Kubo T, Easterling CP, Olson RA, Sumerlin BS (2018) Polym Chem 9:4605
27. Kocak G, Solmaz G, Tuncer C, Bütün V (2019) Europ Polym J 110:364
28. Kıvanç MR, Ozay O, Ozay H, Ilgin P (2020). J Dispers Sci Technol. https://doi.org/10.1080/01932691.2020.1847658
29. Hampejsova Z, Batek J, Sirc J, Hobzova R, Bosakova Z (2019) Monatsh Chem 150:1691
30. Qi Y, Li K, Zhao C, Ma Y, Yang W (2021) J Chem Technol Biotechnol 96:1902
31. Mittal H, Al Alili A, Alhassan SM (2020) Cellulose 27:8269
32. Akti F, Boran F (2016) Acta Phys Pol A 130:147
33. Youssefi Azarfam M, Nasirinezhad M, Naeim H, Zarrintaj P, Saeb M (2021) J Compos Sci 5:125
34. Olad A, Nouri N, Eslamzadeh M (2019) SN Appl Sci 1:868
35. Sanaeepur H, Kargari A, Nasernejad B (2014) RSC Adv 4:63966
36. Wang C, Leng S, Xu Y, Tian Q, Zhang X, Cao L, Huang J (2018) Minerals 8:145
37. Vargün E, Usanmaz A (2010) J Macromol Sci A 47:882
38. Kurecic M, Sfiligoj-Smole M, Stana-Kleinschek K (2012) Mat Technol 46:87
39. Jain A, Bajpai J, Bajpai AK, Mishra A (2020) Polym Bull 77:4417
40. Dave PN, Gor A (2018) Natural polysaccharide-based hydrogels and nanomaterials. In: Hussain CM (ed) Handbook of Nanomaterials for Industrial Applications. Elsevier, p 36
41. Rashidzadeh A, Olad A, Salari D, Reyhanitabar A (2014) J Polym Res 21:344
42. Tatlier M, Munza G, Henninger SK (2018) Microporous Mesoporous Mater 264:70
43. Lee W-F, Huang Y-L (2000) J Appl Polym Sci 77:1769
44. Don T-M, Chou S-C, Cheng L-P, Tai H-Y (2011) J Appl Polym Sci 120:1
45. D'Agostino A, Colella M, de Rosa M, de Rosa A, Lanza A, Schiraldi C (2009) J Polym Res 16:561
46. Tanaka FC, Junior CRF, Fernandes RS, de Moura MR, Aouada FA (2021) J Polym Environ 29:3389
47. Gull N, Khan SM, Zahid Butt MT, Khalid S, Shafiq M, Islam A, Asim S, Hafeez S, Khan RU (2019) RSC Adv 9:31078
48. Charaya H, Li X, Jen N, Chung H-J (2019) Langmuir 35:1526
49. Zohuriaan-Mehr MJ, Kabiri K, Kheirabadi M (2010) J Appl Polym Sci 117:1127
50. Pan A, Roy SG, Haldar U, Mahapatra RD, Harper GR, Low WL, De P, Hardy JG (2019) Gels 5:43
51. Yildiz B, Isik B, Kis M (2002) React Funct Polym 52:3
52. Cicek H, Tuncel A (1998) J Polym Sci A Polym Chem 36:527
53. Shekhar S, Mukherjee M, Sen AK (2012) Adv Mat Res 1:269
54. Mandal S, Roy D, Chaudhari RV, Sastry M (2004) Chem Mater 16:3714
55. Durmuş S, Yilmaz B, Kıvanç MR, Onder A, Ilgin P, Ozay H, Ozay O (2021) Gold Bull 54:75
56. Onder A, Ilgin P, Ozay H, Ozay O (2020) J Environ Chem Eng 8:104436